Received: Added at production | Revised: Added at production | Accepted: Added at production

DOI: xxx/xxxx

ARTICLE

# Uplink Grant-free PDMA Transmission Scheme by Exploiting Poly Complementary Sequence

Shufeng Li*[1] | Baoxin Su[1] | Yao Sun[2] | Sanshan Sun[3] | Libiao Jin[1]

[1]the State Key Laboratory of Media Convergence and Communication, School of Information and Communication Engineering, Communication University of China, Beijing 100024, China
[2]James Watt School of Engineering, University of Glasgow, G12 8QQ, Scotland, U.K.
[3]College of Physics and Electronic Engineering, Sichuan Normal University, Chengdu 610101, China

**Correspondence**
*Shufeng Li, the State Key Laboratory of Media Convergence and Communication, School of Information and Communication Engineering, Communication University of China. Email: lishufeng@cuc.edu.cn

**Present Address**
the State Key Laboratory of Media Convergence and Communication, School of Information and Communication Engineering, Communication University of China, Beijing 100024, China

**Abstract**

Non-orthogonal multiple access (NOMA) technology is a key technology of the future cellular mobile communication system. It provides services for users under different channel conditions through signal superposition transmission and spectrum multiplexing. Pattern division multiple access (PDMA) is a new NOMA technology based on the overall optimization of multi-user communication system. Since the performance of PDMA mainly depends on the gain of the pattern matrix, we propose a design scheme of uplink PDMA pattern matrix for ultra-reliable low latency communication (uRLLC). For the interference between users is a common problem in NOMA system, first, we use poly complementary sequence (PCS) as the spread codebook to spread the PDMA transmission signal and reduce interference. Meanwhile, an uplink power control scheme is proposed. It allocates wireless resources reasonably by jointly considering the interference between users and resource blocks within users (JUR), the corresponding outage probability formula is also derived. Simulation results show that compared with the previous researches, the pattern matrix design scheme and JUR power control scheme proposed in this paper have greatly improved the transmission performance. The addition of PCS spread spectrum technology can significantly reduce the block error rate and outage probability.

**KEYWORDS:**
non-orthogonal multiple access,pattern division multiple access,poly complementary sequences,grant-free, uRLLC,pattern matrix,power control

## 1 | INTRODUCTION

The new multiple access technology is an important candidate technology for the physical layer of the future cellular communication system[1,2]. Non-orthogonal multiple access (NOMA) improves the access capability of the system through signal superimposed transmission, effectively meeting the connection requirements of hundreds of millions of devices in the future wireless network[3,4,5]. NOMA allows different users to occupy the same spectrum, time, space and other resources, which can achieve significant performance gain compared with orthogonal multiple access (OMA) technology[6]. Due to the non-orthogonal allocation of resources, NOMA has a higher overload rate than the traditional OMA, so as to increase the network throughput without affecting the user experience, and meet the needs of 6G massive connection and high frequency spectrum efficiency

[0]**Abbreviations:** PDMA, pattern division multiple access; NOMA, non-orthogonal multiple access; OMA, orthogonal multiple access; SCMA, sparse coded multiple access; MUSA, multi-user shared access; PCS, poly complementary sequences; uRLLC, ultra-reliable low latency communication; UE, user equipment; RB, resource block; SIC, successive interference cancellation; BP, belief propagation; GF, grant-free; CND, channel node; UND, user node; MAP, maximum a posteriori; QPSK, quadrature phase shift keying; CDF, cumulative distribution function; SNR, signal to noise ratio; BLER, block error rate

in the future[7,8]. NOMA is the most promising spectrum access technology for the 6G, which allows the use of same spectrum for multiple users, resulting in higher spectrum efficiency and lower latency[9,10]. Common NOMA technologies include sparse coded multiple access (SCMA), multi-user shared access (MUSA) and pattern division multiple access (PDMA)[11].

As an emerging NOMA technology, PDMA is highly valued by academia and industry, and it is included in the research report of future technology trends by ITU[12]. PDMA is a new type of NOMA with joint optimization design of transmitter side and receiver side. At the transmitter side, the signals of multiple users are mapped to the same time domain, frequency domain and spatial domain resources through the PDMA patterns for multiplexing transmission. Successive interference cancellation (SIC) detection algorithm or belief propagation (BP) detection algorithm is used for multi-user detection at the receiver side[13,14]. Compared with SCMA, PDMA can use multi-dimensional domain to design non-orthogonal feature drawings independently or jointly, make full use of multi-dimensional domain processing, and there is no limit on the number of users sharing the same resources. Therefore, PDMA technology has the advantages of wider application scope and higher flexibility, so we chooses PDMA for research in this paper.

Codebook design is the key technology of all NOMA mechanisms. The codebook of SCMA is based on the joint optimization of sparse spread spectrum and multi-dimensional modulation, and the codebook of MUSA is a short spread spectrum sequence with low cross-correlation. Similarly, in PDMA, the design of pattern matrix has a very important impact on system performance and complexity, which is the key to achieve good system performance. The related design schemes of PDMA pattern matrix include uplink pattern matrix design schemes for minimizing sum squared correlation (SSC) and constellation constrained capacity[15], and pattern matrix design schemes for different application scenarios[16]. However, most existing design schemes cannot be directly used for the matrix design in ultra-reliable low latency communication (uRLLC). To unlock the potentials of PDMA for uRLLC scenario, it is urgently calling for an efficient patter matrix design in PDMA system.

Uplink grant free (GF) transmission can be divided into radio resource control (RRC) connected state and RRC inactive state. When the terminal RRC is in the connected state, strict uplink synchronization is guaranteed by setting before transmission. And through power control, the instantaneous signal-to-noise ratio (SNR) of the receiver is kept constant. Therefore this mode is suitable for uRLLC[17], which can shorten the transmission time interval while ensuring high reliability and reduce user delay. [18][18] studied the performance of GF NOMA transmission in mMTC scenario and evaluated its feasibility, from which we can know that GF transmission can greatly simplify the access link, reduce the control signaling overhead, access delay and terminal consumption. But GF random access causes collision will results in non-orthogonal resource sharing between the user equipments (UEs)[19]. PDMA can naturally be incorporated with GF transmission to reduce the collision probability, intelligently overlapping of the UEs at the transmitter allows to separate them at the receiver[20,21]. Therefore, in this paper we analyze the uplink GF PDMA transmission in the uRLLC scenario.

In NOMA technology, the interference between users is a common problem of the system, it can directly affect the detection complexity and recovery accuracy. Complete complementary sequence is a generalization of Golay complementary codes, which is a set of sequences with ideal correlation sum[22]. As a multi-codebook set in complex field composed of multiple subsequences, the poly complementary sequence (PCS) can achieve zero cross-correlation value and reduce the interference among users by using the complementarity between subsequences[23].[24][24] studied the performance of complete complementary sequence (CCS)-based spread-time code-division multiple access in frequency-nonselective fading channels. It is verified that CCS spread spectrum can improve bit error rate (BER) performance in frequency-nonselective fading channel, so Rayleigh channel is selected for simulation in this paper. [25][25] introduced the polyphase complete complementary code into the integration of spread spectrum radar and communication. The superiority of CCS in related aspects is verified, which means that CCS can be used as spread spectrum sequence in the field of radar and communication integration. [26][26] proposed a solution that exploits complete complementary spectrum spreading and data compression techniques jointly to resolve the communication challenges whilst ensuring efficient use of spectrum and acceptable bit error rate. At present, there is little research on the combination of PCS spread spectrum technology and NOMA transmission, so we select PCS as the spread spectrum code to process the transmission signal of PDMA (PCS-PDMA), which combines the advantages of PCS into PDMA communication system to improve the implementation of NOMA communication.

With the rapid growth of data traffic and the number of mobile users, the allocation of limited wireless network resources has become an important issue[27,28]. In uplink NOMA, multiple users transmit non-orthogonal signals on the same resource block (RB) to the base station, and each UE transmits its signal independently with the maximum transmission power or controlled transmission power[29]. In [30][30], the problem of joint relay selection and max-min energy-efficient power allocation in downlink multicell NOMA networks is studied. In order to meet the quality of service constraints and achieve maximum minimum energy efficiency, it performs relay selection for each cellular user in each cell. [31][31] proposed an iterative power allocation algorithm

to optimize the power allocation of dowmlink PDMA. It uses karush Kuhn tucher condition to increase the system throughput and optimize the system performance. [32][32] through the calculation of the column weight ratio of the PDMA pattern, a power control scheme based on the PDMA pattern is proposed. However, in the PDMA uplink transmission system, multiple users are superimposed in the power domain and different users have the same expected received power at the base station. The power allocation to one UE will also affect the channel quality of other UEs in this system[33,34]. Therefore, it is particularly important to use the appropriate power control scheme. In order to reduce the interference, we optimized the power control scheme of [32][32] and proposed a new PDMA power control scheme by jointly considering the interference between UEs and RBs within users (JUR).

The main contributions of this paper are summarized as follows:

- A new pattern matrix design scheme of the uplink PDMA uRLLC is proposed. By jointly considering the repetitiveness of the binary basic pattern, SSC, pattern diversity and the weighted row weight, a performance evaluation factor of pattern matrix is set to improve the performance of PDMA system.
- An uplink JUR power control scheme of PDMA is proposed. Considering the interference between UEs and RBs within each user in PDMA, we set the transmit power control factor to allocate wireless resources reasonably and the corresponding outage probability formula is derived.
- We use PCS as the spread spectrum sequence, combined with PDMA transmission performance, to spread spectrum signal processing. Utilize the complementarity between sub-sequences to achieve zero cross-correlation value, reduce the interference between users, and improve the performance of the system.

The rest of this paper is organized as follows. Section 2 introduces the PCS-PDMA uplink transmission system model. Section 3 introduces the pattern matrix design scheme for uRLLC. Section 4 analyzes the transmission rate and outage probability of the uplink PDMA JUR power control scheme. In section 5, the performance of the design scheme is discussed in detail through simulation. Finally, we will summarize the full text in section 6.

## 2 | SYSTEM MODEL OF UPLINK PCS-PDMA TRANSMISSION

The basic idea of PDMA technology is based on the joint design of transmitter and receiver side. Figure 1 shows the system model of PCS-PDMA uplink system, in which the transmitter and receiver side use a single antenna. At the transmitter side, the PDMA encoder maps the PCS spread spectrum signal of multi-user to the corresponding RB according to the pattern matrix, and generate the PDMA modulation vector. At the receiver side, the despread signal is detected by advanced receiving technologies such as SIC and BP algorithm to separate the superimposed signals.

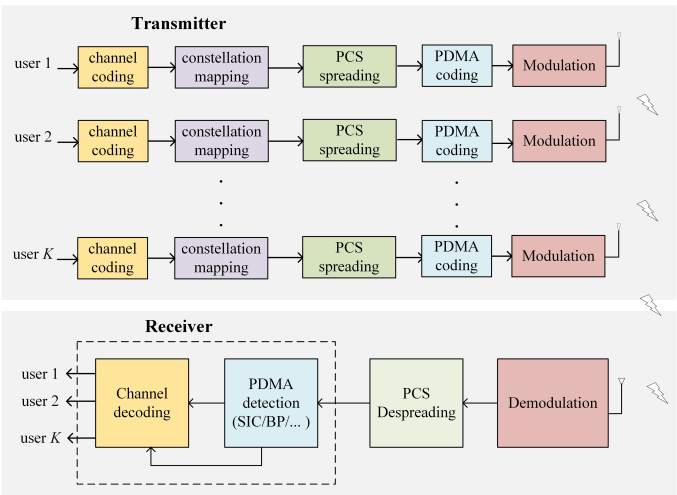


**FIGURE 1** PCS-PDMA uplink transmission system model.

In this system, $K$ user data is mapped to $N$ RBs through different feature patterns $f_k$, and the PDMA modulation vector $v_k$ of the $k$-th UE is

$$v_k = f_k x_k \ , \quad 1 \le k \le K, \tag{1}$$

where $x_k$ is the transmission signal of the $k$-th UE, $f_k$ is the binary vector of $[N \times 1]$ and contains elements "1" and "0", to indicate that the element is mapped to the corresponding RB or not. The PDMA pattern matrix is represented by $F_{PDMA}^{[N\times K]}$, and $F_{PDMA}^{[N\times K]} = \left[f_1, f_2, ..., f_K\right]$.

The received signal of base station is given by

$$y = \sum_{k=1}^{K} diag\left(h_k\right) v_k + n, \tag{2}$$

where $n$ is the received interference and noise, $h_k$ is the channel response of the $k$-th UE, and $diag\left(h_k\right)$ is the diagonal matrix with element $h_k$. Equation (2) can be simplified as

$$y = Hx + n, \tag{3}$$

where $x = \left[x_1, x_2, ..., x_K\right]^T$ and $H$ denote the equivalent channel response matrix of $K$ UEs multiplexed on $N$ RBs, $H = H_{CH} \odot F_{PDMA}^{[N\times K]}$ and $H_{CH} = \left[h_1, h_2, ..., h_K\right]$ is rayleigh channel response matrix. Therefore, equation (3) can be expressed as

$$\begin{aligned} y &= H_{CH} \odot F_{PDMA}^{[N\times K]} x + n \\ &= \left[h_1, h_2, ..., h_K\right] \odot F_{PDMA}^{[N\times K]} \left[x_1, x_2, \cdots, x_k\right]^T + n. \end{aligned} \tag{4}$$

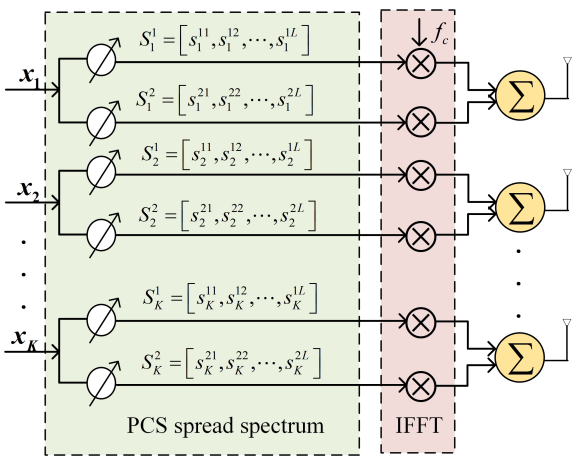


**FIGURE 2** PCS model structure.

Complete complementary sequences are composed of mutually orthogonal complementary sequences. Different from the traditional single codebook spreading sequence, the complete complementary sequence is a multi-codebook joint design scheme, using the principle of complementary correlation between subsequences of multiple codebooks to obtain a sequence with a cross-correlation value of zero, eliminating the interference between users. Due to the limited number of codebook of the binary sequence and the unsatisfactory cross-correlation function, thus we choose PCS as the spread spectrum sequence[35]. Figure 2 is the structure of PCS model.

The set of PCS can be expressed as $S_k = \left(S_k^1, S_k^2\right)$. $S_k^1$ and $S_k^2$ is a pair of complementary sequences with length $l$. Their aperiodic autocorrelation function is $2l$ when the transmission delay is zero, and satisfy the complete orthogonality. $S_k^1$ and $S_k^2$ encode the user data in turn, and the $k$-th spread spectrum sequence is given by

$$\begin{aligned} m_k(t) &= iffft\left(S_k^1(t) + S_k^2\left(t - \tau_0\right)\right) \\ &= iffft\left\{\sum_{l=0}^{L-1}\left[s_k^{1l} rect\left(\frac{t-(l+1)T_c}{LT_c}\right) + s_k^{2l} rect\left(\frac{t-(l+1)T_c-\tau_0}{LT_c}\right)\right]\right\}, \end{aligned} \tag{5}$$

where $T_c$ is the chip period, $T_c = 1/f_c$, $\tau_0$ is the transmission time delay, and $rect$ is the rectangular window function.

The received signal of PCS spread spectrum is given by

$$y(t) = \sum_{k=1}^{K} diag\left(h_k\right) f_k x_k m_k(t) + n. \tag{6}$$

At the receiver side, BP detection algorithm requires message exchanges between the channel node (CND) and the user node (UND) through the edges of the factor graph, and make the best decision once reaching a stable value after multiple iterations. Belief propagation detection algorithm is also known as the message passing algorithm, which has good performance of approaching the maximum a posteriori (MAP) detection algorithm. The sparsity of the PDMA pattern matrix can greatly reduce the complexity of the BP algorithm.

Given the PDMA receiver side signal $y$ and the multi-user equivalent channel response matrix $H$ of the base station, the optimal detection algorithm of modulation symbol $x$ transmitted by PDMA multi-user is MAP detection. The joint map optimal solution is formulated as

$$\hat{x} = \arg\max p(x|\, y, H), \tag{7}$$

where equation (7) is approximated by the local MAP optimal solution. Using Bayesian formula, we can get

$$\hat{x}_k = \arg\max_{s\in\aleph_k} \sum_{x, x_k = s} P(x) \prod_{n\in N_v(k)} p\left(y_n \middle| x\right), \tag{8}$$

where $\aleph_k$ represents the set of constellation points of the $k$-th UE, $N_v(k)$ is the sequence number set of time-frequency resources mapped by the $k$-th UE's PDMA pattern.

The external information is a measure of soft information, representing the reliability of each edge connecting CND and UND, and is generally defined by log likelihood ratio. The BP algorithm obtains posterior information by iteratively processing the exchanges between CND and UND. Figure 3(a) shows the CND message processing process during BP iteration. The external information sent by the UND $x_k$ to the CND $y_j$ in the $l$-th iteration is

$$L^l_{x_k\to y_j}\left(x_k = s\right) = \sum_{j'\in N_v(k)\backslash j} L^{l-1}_{x_k\leftarrow y_{j'}}\left(x_k = s\right), \tag{9}$$

where $L^l_{x_k\leftarrow y_j}(x = s)$ is the external information transmitted by $y_j$ to $x_k$ at the $l$-th iteration, $s$ is the modulation symbol, and $N_v(k)$ is the set of all CND connected with $x_k$.

Figure 3(b) shows the CND message processing process during BP iteration. In the $l$-th iteration, the external information transmitted by CND $y_j$ to UND $x_k$ is given by

$$\begin{aligned} L^l_{x_k\leftarrow y_j}\left(x_k = s\right) &= \ln \frac{E\left\{ p\left(y_j \middle| x\right) \middle| x_k = s, \left\{ L^l_{x_{k'}\to y_j}\left(x_{k'}\right), k' \in N_c(j) \middle| k \right\} \right\}}{E\left\{ p\left(y_j \middle| x\right) \middle| x_k = s_0, \left\{ L^l_{x_{k'}\to y_j}\left(x_{k'}\right), k' \in N_c(j) \middle| k \right\} \right\}} \\ &= \ln \frac{\sum\limits_{x_{N_c(j)\backslash k}, x_k = s} p\left(y_j \middle| x\right) \cdot \prod\limits_{k'\in N_c(j)\backslash k} p\left(x_{k'}\right)}{\sum\limits_{x_{N_c(j)\backslash k}, x_k = s_0} p\left(y_j \middle| x\right) \cdot \prod\limits_{k'\in N_c(j)\backslash k} p\left(x_{k'}\right)}, \end{aligned} \tag{10}$$

where $N_c(j)$ represents the set of all UND connected to $y_j$.

The max-log algorithm is formulated as

$$\log\left(e^a + e^b\right) \approx \max(a, b). \tag{11}$$

Equation (10) can be approximately simplified to

$$\begin{aligned} L^l_{x_k\leftarrow y_j}\left(x_k = s\right) \simeq & \max_{x_{N_c(j)\backslash k}, x_k = s} \left\{ -\frac{1}{2\sigma^2}\left|y_j - h_j^T x\right|^2 + \sum_{k'\in N_c(j)\backslash k} L^l_{x_{k'}\to y_j}\left(x_{k'}\right) \right\} - \\ & \max_{x_{N_c(j)\backslash k}, x_k = s_0} \left\{ -\frac{1}{2\sigma^2}\left|y_j - h_j^T x\right|^2 + \sum_{k'\in N_c(j)\backslash k} L^l_{x_{k'}\to y_j}\left(x_{k'}\right) \right\}, \end{aligned} \tag{12}$$

where $h_j$ is the $j$-th column of the equivalent channel response matrix $H$, and $\sigma^2$ is the complex Gaussian noise power.

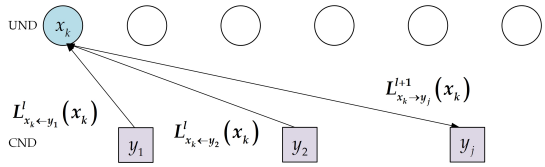


(a) Message processing of UND

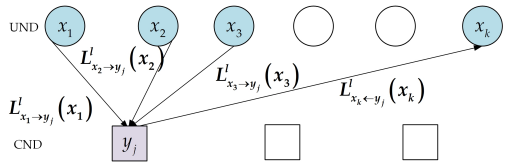


(b) Message processing of CND

**FIGURE 3** PDMA pattern matrix message processing process.

When the iteration satisfies the convergence condition, the posterior information $L^D\left(x_k = s\right)$ of the variable node can be calculated by equation (13) for decoding operation.

$$L^D\left(x_k = s\right) = \sum_{j' \in N_V(j)} L^{L_{\max}}_{x_k \leftarrow y_{j'}}, x_k = s. \tag{13}$$

## 3 | PDMA PATTERN MATRIX DESIGN FOR URLLC

As one of the important communication scenarios, uRLLC has high requirements of delay and reliable transmission. It is necessary to reduce the transmission delay, network forwarding delay and retransmission probability as much as possible in uRLLC. The introduction of a new multiple access technology that supports GF can further reduce the signaling overhead and data transfer of uRLLC[36].

PDMA pattern defines the mapping rules of data flow to RB. The traditional method is to use binary vector to represent, assign different patterns to each user, and combine all user's patterns into a pattern matrix. Figure 4 shows the PDMA multi-user pattern mapping corresponding to $F^{[3\times6]}_{PDMA}$. When the vector element $f_{n,k}$ in the pattern is '1', the data of the $k$-th UE is mapped to the $n$-th RB and '0' otherwise. The overload rate can be expressed as

$$\lambda = \frac{K}{N}. \tag{14}$$

On the basis of time-domain transmission, we can further consider optimizing the PDMA pattern in the power domain to improve the transmission performance, by introducing the power factor and phase rotation factor into the PDMA pattern matrix. When the signal is modulated by QPSK, the constellation distribution is not uniform, and the constellation points and input user data are no longer one-to-one mapping[37]. In order to solve this ambiguity, it is necessary to add power scaling and phase shift factors into PDMA pattern matrix.

$$g_{n,k} = \beta_{n,k} f_{n,k} e^{-j\varphi_{n,k}}, \tag{15}$$

where $\beta_{n,k}$ and $\varphi_{n,k}$ respectively represent the transmit power ratio and phase rotation factor allocated by the $k$-th UE on the $n$-th RB, $G^{[N\times K]}_{PDMA} = \left[g_1, g_2, \cdots, g_K\right]$. As the randomness of the phase rotation factor is stronger, it is more conducive to multi-user detection at the receiver side, hence we choose random phase to design.

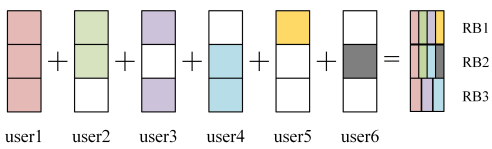


**FIGURE 4** Multi-user mapping of $F^{[3\times6]}_{PDMA}$.

The energy scaling and phase transformation can replace the "1" in the PDMA original matrix, and naturally combine into the PDMA pattern matrix to reflect the energy scaling and phase shift. In uplink PDMA, the transmission power of each user is limited, and it satisfies equation (16).

$$\sum_{n=1}^{N} \left\| g_{n,k} \right\|^2 = 1 \ , k = 1, 2, \cdots, K. \tag{16}$$

It is necessary to minimize the interference between patterns and avoid the mode with large load in uRLLC. The complexity of multi-user detection also needs to be considered in the design process of PDMA pattern matrix. The complexity of BP detection algorithm depends on the maximum row weight $d_{\mathrm{r-max}}$ and modulation order $M$ of PDMA pattern matrix, and the complexity can be expressed as $O\left(2^{M d_{r-\max}}\right)$.

Let

$$G^0 = ceil\left(G_{PDMA}^{[N\times K]}\right) = \left[g_1^0, g_2^0, \cdots, g_K^0\right] = \left[g_1'^0, g_2'^0, \cdots, g_N'^0\right]^T, \tag{17}$$

where $ceil$ denotes rounding in the direction of positive infinity. $d_{\mathrm{r-max}}$ is given by

$$d_{r-\max} = \max\left(\sum_{k=1}^{K} g_k^0\right). \tag{18}$$

The design criteria of PDMA pattern matrix mainly include the following points:

- Minimize the repeatability of the binary original patterns corresponding to the pattern matrix to reduce the interference between users.

$$r = \max\left[rep\left(g_1^0, g_1^0, \cdots, g_K^0\right)\right], \tag{19}$$

  where $rep$ is the number of repeated patterns.

- Minimize SSC to reduce the correlation between patterns and increase the sparsity, which is beneficial to multi-user detection at the receiver side.

$$SSC = \sum_{k=1}^{K} \sum_{k'=1, k'\neq k}^{K} abs\left(g_k^H g_{k'}\right)^2. \tag{20}$$

- Minimize the maximum weighted row weight to reduce the complexity of multi-user detection at the receiver side. In this case, the PDMA mode matrix can calculate the weighted maximum row weight $d_{r-\max}^{w}$ by considering each reused RB.

$$d_{\mathrm{r-max}}^{w} = \sum_{n=1}^{N}\left(\frac{1}{2}\sum_{k=1}^{K}\left[\left\|g_{n,k}\right\|^2\right]\left(\sum_{k=1}^{K}\left[\left\|g_{n,k}\right\|^2\right] - 1\right)\right). \tag{21}$$

- Maximum diversity to accelerate the convergence speed of BP detector.

$$div = \max\left(\sum_{n=1}^{N} g_n'^0\right), \tag{22}$$

The correlation coefficient $\rho$ between patterns is formulated as

$$\rho = \frac{\sum_{k=1}^{K}\sum_{k'=1}^{K}\left(g_k - \bar{g}_k\right)\left(g_{k'} - \bar{g}_{k'}\right)}{\sqrt{\sum_{k=1}^{K}\left(g_k - \bar{g}_k\right)^2}\sqrt{\sum_{k'=1}^{K}\left(g_{k'} - \bar{g}_{k'}\right)^2}}. \tag{23}$$

The specific flow of the design algorithm of the uplink PDMA pattern matrix for uRLLC is shown in algorithm 1.

The comprehensive performance evaluation factor of the PDMA pattern matrix is given by

$$Q = \frac{SSC \cdot d_{r-\max}^{w}}{div}. \tag{24}$$

The obtained PDMA pattern matrix of different dimensions for uRLLC is shown in Table 1.

**Algorithm 1** Uplink PDMA pattern matrix design algorithm for uRLLC

**Step1**: Given the number of RB, $N$. Get $F^{[N\times K]}$ which consists of $F^{[N\times K]}$ patterns.
**Step2**: The distribution of $\beta_{n,k}$ satisfies equation (16), and $\varphi_{n,k}$ is completely random.
**Step3**: Set correlation coefficient threshold, $\rho_{th}$. The correlation coefficient $\rho$ between any two patterns in $F^{[N\times K]}$ is calculated by equation (23), the patterns whose $\rho \leq \rho_{th}$ are selected. Get a combination of patterns, where the $\rho$ between any pair of patterns is less than $\rho_{th}$.
**Step4**: Set the overload rate, $\lambda$. Through the following process to traverse $I$ pattern combinations ($pt$), and get several pattern matrices with dimension $(N \times \lambda N)$.
**for** $i$=1:$I$ **do**
  **if** pattern number $u_i \geq \lambda N$ in $pt_i$ **then**
    Taking the diversity ($div$) as the index, the pattern matrix with dimension $(N \times \lambda N)$ is selected from the pattern combination.
  **else** Select multiple groups of $(\lambda N - u)$ patterns from the pattern combination $pt_i$, and form a matrix of multiple $(N \times \lambda N)$ with them, select the pattern matrix with the smallest $d^{w}_{r-\max}$.
  **end if**
**end for**
**Step5**: Calculate SSC, $d^{w}_{r-\max}$ and $div$ of the previously selected matrix respectively, and calculate the comprehensive performance evaluation factor $Q_i$ by equation (24). The pattern matrix with the smallest $Q$ is the result.

**TABLE 1** PDMA design pattern matrix of different dimensions.

| Dimension | Pattern Matrix | SSC | $d^{w}_{r-\max}$ | *div* | *Q* |
|---|---|---|---|---|---|
| $2\times 3$ | $\begin{bmatrix} -0.7071 & -i & 0 \\ -0.7071i & 0 & -1 \end{bmatrix}$ | 1 | 0.7500 | 2 | 0.3750 |
| $3\times 6$ | $\begin{bmatrix} 0.5774 & 0 & 0 & 0 & i & -1 \\ 0.5774 & 0.7071 & 0 & 1 & 0 & 0 \\ -0.5774 & 0.7071 & 1 & 0 & 0 & 0 \end{bmatrix}$ | 3.3333 | 3.0833 | 3 | 3.4259 |
| $4\times 6$ | $\begin{bmatrix} -0.5 & 0.5774i & 0.7071i & 0 & 0 & 0 \\ 0.5 & 0 & 0.7071i & 0 & 0 & 1 \\ 0.5i & -0.5774i & 0 & 0 & -1 & 0 \\ 0.5 & 0.5774i & 0 & -i & 0 & 0 \end{bmatrix}$ | 2.1667 | 1.6521 | 4 | 0.8803 |
| $4\times 8$ | $\begin{bmatrix} 0.5i & -0.5774i & 0 & -0.7071 & -0.7071i & 0 & 0 & -i \\ -0.5i & 0 & -0.7071i & 0 & 0 & 0 & -1 & 0 \\ -0.5 & 0.5774i & 0.7071 & 0 & -0.7071 & 0 & 0 & 0 \\ -0.5 & 0.5774 & 0 & 0.7071i & 0 & 1 & 0 & 0 \end{bmatrix}$ | 4.3257 | 4.0139 | 4 | 4.3407 |

## 4 | JUR POWER CONTROL SCHEME OF PDMA

In order to reduce the interference between UEs and RBs within users of PDMA and allocate resources reasonably, we propose a JUR power control scheme of PDMA.

Given $\alpha_{n,k}$ as the target received power proportional control factor of the $k$-th UE on the $n$-th RB. Suppose that user 1 to user $K$ represent a group of UE from the nearest to the farthest of the base station, and channel gain $|h_{n,1}| \geq |h_{n,2}| \geq \cdots \geq |h_{n,K}|$[38]. Considering the perceived quality of service, user 1 is assigned to the PDMA pattern with the largest column weight, and the target receiving power transmitted by user 1 on its occupied $c_1$ RB is the expected receiving power. The scaling factor of the $k$-th UE when transmitting on the $c_k$ RB can be expressed as $w_k = \frac{c_k}{c_1}$. Since the power allocation of each UE will affect the transmission of other UE, the number of UEs on each RB should be considered at this time. Let $b_n$ represent the number of UE

multiplexing the $n$-th RB. Then the power scaling factor can be expressed as

$$\alpha_{n,k} = w_k \frac{1}{b_n} = \frac{c_k}{c_1 b_n}. \tag{25}$$

The transmission power of the $k$-th UE is formulated as

$$P_k = \alpha_k P_u = \sum_{i=1}^{N} \alpha_{i,k} P_u = \frac{c_k}{c_1} \sum_{i=1}^{N} \frac{1}{b_i} P_u, \tag{26}$$

where $P_u$ is the expected received power of each UE.

The signal received by the base station is given by

$$y = h_k g_k \sqrt{P_k} x_k + \sum_{a \neq k}^{K} h_a g_a \left( \sqrt{P_a} x_a \right) + n \ , k \in [1, K]. \tag{27}$$

The receiving signal of PCS spread spectrum can be further expressed as follows.

$$y(t) = \sum_{k=1}^{K} diag\left(h_k\right) g_k \left( \sqrt{P_k} x_k \right) m_k(t) + n \ , \tag{28}$$

where $k \in [1, K]$ and $i \in \{1, 2\}$.

## 4.1 | Transmission rate analysis

The SINR of the $k$-th UE is given by

$$\begin{aligned} SINR_k =& P_k \left(g_k\right)^H \left( N_0 + \sum_{i \neq k}^{K} P_i g_i \left(g_i\right)^H \right)^{-1} g_k \\ =& \alpha_k P_u \left(g_k\right)^H \left( N_0 + \sum_{i \neq k}^{K} \alpha_i P_u g_i \left(g_i\right)^H \right)^{-1} g_k, \end{aligned} \tag{29}$$

where $P_k$ represents the transmit power of user $k$, $N_0$ represents power noise, and $\alpha_k = \sum_{n=1}^{N} \alpha_{n,k}$.

The transmission rate of $k$-th UE can be expressed as

$$\begin{aligned} r_k =& \log_2 \left( 1 + P_k \left(g_k\right)^H \left( N_0 + \sum_{i \neq k}^{K} P_i g_i \left(g_i\right)^H \right)^{-1} g_k \right) \\ =& \log_2 \left( 1 + \sum_{n=1}^{N} \alpha_{n,k} P_u \left(g_k\right)^H \left( N_0 + \sum_{i \neq k}^{K} \sum_{n=1}^{N} \alpha_{n,i} P_u g_i \left(g_i\right)^H \right)^{-1} g_k \right). \end{aligned} \tag{30}$$

## 4.2 | Outage probability analysis

Define $A_k = \left\{ r_k < r'_k \right\}$ as the transmission data set of the $k$-th UE that the base station cannot detect, $r'_k$ is the target transmission rate, and $\bar{A}_k$ is the complement of $A_k$, then we have

$$\begin{aligned} p\left(\bar{A}_k\right) =& 1 - p\left\{A_k\right\} \\ =& 1 - p\left\{\log\left(1 + SINR_k\right) < r'_k\right\}. \end{aligned} \tag{31}$$

Let $\eta_k = 2^{r'_k} - 1$ denote the target SINR of the $k$-th UE. Equation (31) is given by

$$\begin{aligned} p\left(\bar{A}_k\right) =& 1 - p\left\{SINR_k < \eta_k\right\} \\ =& 1 - p\left\{ \sum_{n=1}^{N} \alpha_{n,k} P_u \left(g_k\right)^H \left( N_0 + \sum_{i=k+1}^{K} \sum_{n=1}^{N} \alpha_{n,i} P_u g_i \left(g_i\right)^H \right)^{-1} g_k < \eta_k \right\}. \end{aligned} \tag{32}$$

The prerequisite for the base station to successfully detect the data of the $k$-th UE is that it has successfully detected and ideally deleted the interference of the previous ($k$-1) UE. The outage probability of the $k$-th UE is given by

$$\begin{aligned} p_{k-out} =& 1 - p\left(\bar{A}_1 \cap \bar{A}_2 \cap \cdots \cap \bar{A}_{k-1}\right) \\ =& 1 - \prod_{i=1}^{k} p\left\{\bar{A}_i\right\}. \end{aligned} \tag{33}$$

In order to verify the universality, we take the $3\times6$ pattern matrix in **Table 1** as an example to deduce. The outage probability of user 1 can be expressed as

$$\begin{aligned} p\left(\bar{A}_1\right) =& 1 - p\left\{1 + SINR_1 < \eta_1\right\} \\ =& 1 - p\left\{\sum_{n=1}^{N} \alpha_{n,1} P_u \left(g_1\right)^H \left(N_0 I_N + \sum_{i=2}^{K}\sum_{n=1}^{N} \alpha_{n,i} P_u g_i \left(g_i\right)^H\right)^{-1} g_1 < \eta_1\right\}. \end{aligned} \tag{34}$$

The detailed calculation to $p\left(\bar{A}_1\right)$ can be found in **Appendix**.

The outage probability of UE 1 is given by

$$p_{out-1} = 1 - P\left(\bar{A}_1\right). \tag{35}$$

The outage probability of other UE can be expressed as follows.

$$p_{out-k} = 1 - \left(1 - p_{out-1}\right) \exp\left(-\frac{\eta}{uv}\sum_{i=2}^{k}\frac{1}{\alpha_i}\right) \quad , k \neq 1. \tag{36}$$

## 5 | SIMULATION RESULTS AND DISCUSSIONS

In this section, we choose to simulate and verify the PDMA pattern matrix design scheme and JUR power control scheme proposed in this paper under the scenario of GF URLLC. The parameter values involved in the simulation are shown in Table 2.

**TABLE 2** Simulation parameter settings.

| **Simulation Parameters** | **Numerical Value** |
|---|---|
| Carrier | 2 GHZ |
| System bandwidth | 10 MHZ |
| Channel Model | Rayleigh channel |
| Patten matrices | In Table 1 |
| Overload rate | 150%, 200% |
| Modulation | QPSK |
| Modulation Order - $M$ | 4 |
| Iterations - $t$ | 20 |
| Lengtn of PCS sequence | 10 |
| SINR threshold - $\eta$ | 1 |
| $e_1$ in [16] | $\begin{bmatrix} 1 & 0 & 0 & 0 & 0 & 1 \\ 0 & i & 0 & 0 & 0 & i \\ 0 & 0 & 1 & 0 & 1 & 0 \\ 0 & 0 & 0 & i & 0 & 0 \end{bmatrix}$ |
| $e_2$ in [16] | $\begin{bmatrix} 1 & 0 & -0.25+0.433i & 0.354+0.354i & -0.289i+0.5i & 0 \\ 0 & 0 & 0.25+0.433i & -0.5i & 0.577 & 0.577 \\ 0 & 0 & 0.5 & 0.354+0.354i & 0.577 & 0.577 \\ 0 & i & -0.25+0.433i & -0.5 & 0 & -0.289i-0.5i \end{bmatrix}$ |

## 5.1 | Simulation analysis of PDMA pattern matrix design

Figure 5 compares the BLER performance of the PDMA pattern matrix designed in **Table 1** with their corresponding binary matrices. It can be seen from the simulation results in Figure 5 that the BLER of the design pattern matrix is smaller and the performance is much better. In theory, adding power scaling factor and phase rotation factor can reduce the mapping ambiguity between constellation points and users, the performance of design matrix should be better than that of binary matrix.

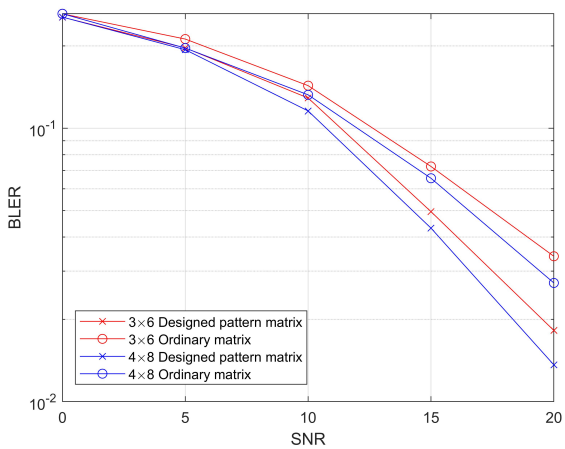


**FIGURE 5** BLER of the designed pattern matrix and the corresponding binary matrix.

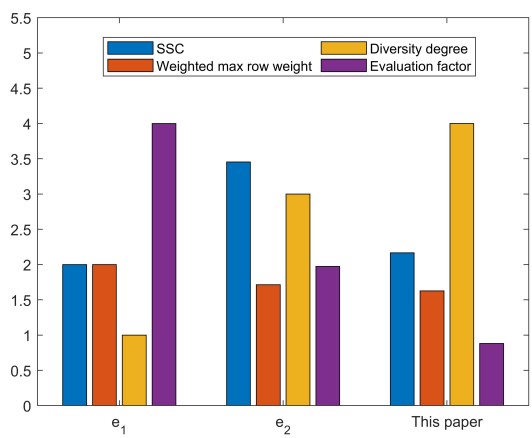


**FIGURE 6** Comparison of important parameters of pattern matrices.

The pattern matrices of type 5 and type 6 proposed in [16][16] are $e_1$ and $e_2$ respectively. We use these matrices to compare with the $4\times6$ pattern matrix in **Table 1**, and calculated SSC, $d^{w}_{r-\max}$, $div$ and comprehensive performance evaluation factor $Q$ of this three matrices. It can be seen from Figure 6 that compared with $e_1$ and $e_2$, the comprehensive performance evaluation factor of the pattern matrix designed in this paper is greatly reduced. The SSC and $d^{w}_{r-\max}$ are smaller, which can effectively increase the sparsity; the $div$ is greater , which is conducive to multi-user detection at the receiver side.

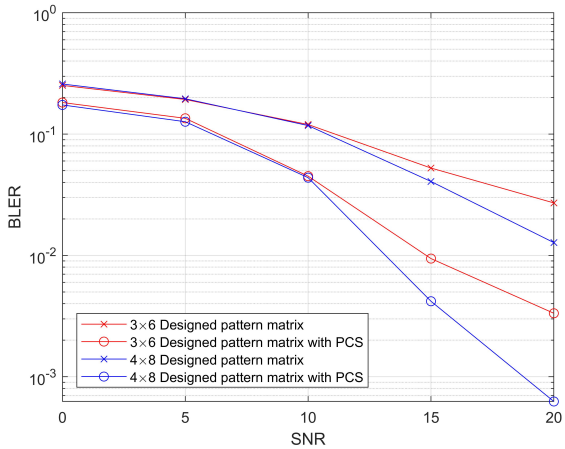


**FIGURE 7** Performance comparison of pattern matrix with PCS spread spectrum.

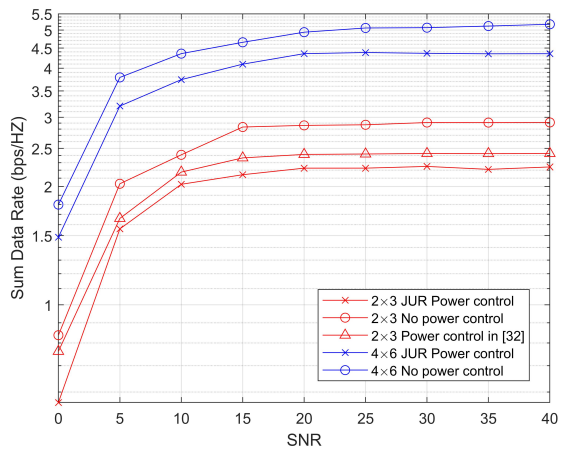


**FIGURE 8** Transmission rate of PCS with and without power control.

Figure 7 shows the performance of BLER with PCS spread spectrum. The length of the PCS sequence is 10. It can be seen from the figure that the BLER performance is optimized by adding PCS in the same dimension matrix. As the spread spectrum communication technology expands the signal bandwidth with spread spectrum sequence, it has stronger anti-noise interference performance under the condition of the same SNR. As for PCS, it has perfect non-periodic correlation characteristics, so the system performance can be greatly optimized by combining PCS and PDMA communication technology.

## 5.2 | Simulation analysis of JUR power control scheme

Figure 8 shows the comparison of the sum transmission rate of the power control schemes. We choose $2 \times 3$ and $4 \times 6$ matrices in **Table 1** for analysis, and compare with the control scheme proposed in [32][32] with $2 \times 3$ dimension matrix. The simulation results show that the rate can converge at the SNR of 15dB. Compared with the scheme in [32][32], the sum rate loss of the $2 \times 3$ pattern matrix is about 6.34%. With the addition of power control scheme, the pattern matrix of different dimensions will have a certain degree of rate loss. Theoretically, that is because the power transmitted by users will be reduced with power control, so a part of transmission rate will be lost correspondingly.

Figure 9 shows the outage probability of different power control schemes. Where u1 represents user 1, "Type1" is the JUR power control scheme, "Type2" is the power control scheme proposed in [32][32], and "Type3" is the transmission scheme without power control. Since it has been verified in [32][32] that a lower SINR threshold can achieve better performance, a simulation of

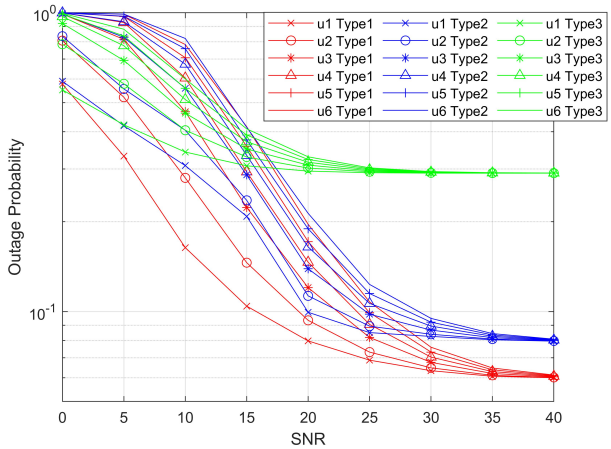


**FIGURE 9** Outage probability of different power control schemes.

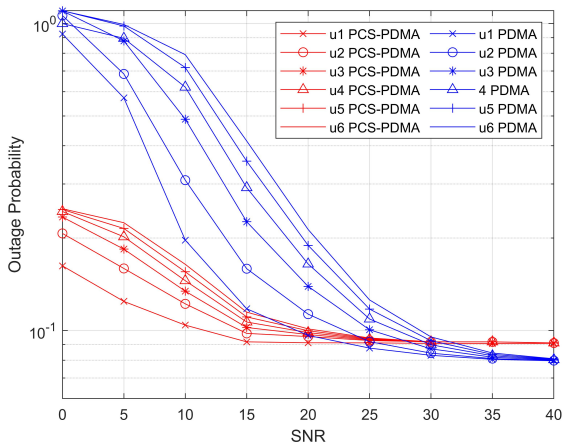


**FIGURE 10** Outage probability of PCS spread spectrum.

the low SINR threshold is carried out in this paper. In the case of SNR less than 10dB scenario, the outage probability of the three schemes has no obvious differences due to the large proportion of interference signals. When SNR is 10-30dB, the outage probability decreases significantly. When the outage probability is $10^{-1}$, the gain of Type 1 is about 4.29dB compared with Type 2, and the performance is obviously improved. When the SNR is higher than 30dB, the outage performance of the three schemes tends to converge. In this case, the outage performance of Type 1 is obviously better than that of Type 2.

Considering the transmission rate in Figure 8 and outage probability in Figure 9 jointly, compared with Type 2, Type 1 loses nearly 6.34% of the transmission rate in exchange for an outage probability gain of nearly 4.29dB. Therefore, the performance of the JUR power control scheme is significantly improved.

Figure 10 simulates the outage probability of JUR power control scheme adding PCS spread spectrum. The length of the PCS sequence is 10 and choose the design pattern matrix with dimension of $3\times6$ in **Table 1**. Compared with the non spread spectrum processing system, the outage performance of PCS spread spectrum is significantly improved when the SNR is lower than 25dB. When the outage probability is $10^{-1}$, a gain of about 7.42dB can be obtained after PCS spread spectrum. This is because the spread spectrum technology can effectively improve the transmission reliability under low SNR. When the SNR is more than 25dB, the performance of the two systems is almost the same and tends to converge. Therefore, outage performance of PCS can be improved significantly in the case of low SNR, which can effectively improve the reliability of the transmission system.

## 6 | CONCLUSION

In this paper, we proposed a PDMA pattern matrix design scheme for uRLLC. Combined with the performance of uplink GF PDMA transmission, the PCS spread spectrum transmission and JUR power control schemes are proposed to reduce the interference. First, in the design scheme of pattern matrix proposed for uRLLC, we comprehensively consider the binary original pattern repetition rate, SSC, weighted maximum row weight and diversity, and set the comprehensive performance evaluation factor. Compared with the previous design scheme, the performance of the pattern matrix designed in this paper is significantly improved. Second, considering the interference in PDMA, a PCS-PDMA spread spectrum transmission scheme is proposed. Considering the interference between UEs and RBs within users in PDMA, a JUR power control scheme is proposed. The corresponding outage probability formula is derived. Compared with the previous researches, the JUR power control scheme obtains an outage probability gain of nearly 4.29dB at the cost of a transmission rate loss of nearly 6.34%. In the low SNR (less than 25dB) scenario, the outage probability performance of PCS spread spectrum is greatly improved, and the outage probability gain of PCS spread spectrum is about 7.42dB.

## Appendix A

**TABLE 3** Parameters in this paper.

| Parameters | Assumptions | Parameters | Assumptions |
|---|---|---|---|
| $F$ | PDMA pattern matrix | $d^{w}_{\mathrm{r-max}}$ | weighted maximum row weight |
| $N$ | the number of RBs | $div$ | diversity |
| $K$ | the number of UEs | $Q$ | performance evaluation factor |
| $\lambda$ | overload rate | $\alpha_{n,k}$ | power scaling factor |
| $x$ | transmitting signals | $P_k$ | transmission power of $k$-th UE |
| $y$ | receiving signals | $r_k$ | transmission rate of $k$-th UE |
| $n$ | noise | $\eta_k$ | target SINR |
| $S$ | PCS | $p_{out-k}$ | outage probability of $k$-th UE |

## Appendix B

The calculation to $p\left(\bar{A}_1\right)$.

$$\begin{aligned}
&\alpha_1 P_u\left(g_1\right)^H\left(N_0+\sum_{i=2}^{K}\alpha_i P_u g_i\left(g_i\right)^H\right)^{-1} g_1\\
=&\theta_1+\theta_2+\theta_3+\theta_4+\theta_5\\
=&\frac{\alpha_1 g_{11}^2 \upsilon}{1+\alpha_5 g_{15}^2 \upsilon+\alpha_6 g_{16}^2 \upsilon}+\frac{\alpha_1 g_{21}^2 \upsilon}{1+\alpha_2 g_{22}^2 \upsilon+\alpha_4 g_{24}^2 \upsilon}+\frac{\alpha_1 g_{21}^2 \upsilon}{1+\alpha_2 g_{22} g_{32} \upsilon}\\
&+\frac{\alpha_1 g_{31}^2 \upsilon}{1+\alpha_2 g_{22} g_{32} \upsilon}+\frac{\alpha_1 g_{31}^2 \upsilon}{1+\alpha_2 g_{32}^2 \upsilon+\alpha_3 g_{33}^2 \upsilon}.
\end{aligned} \tag{37}$$

In order to get the solution to equation (37), we need to get the cumulative distribution function (CDF) first. The CDF of $\theta_1$ can be expressed as

$$\begin{aligned} F_{\theta_1}\left(\eta_1\right) =& p\left(\theta_1 < \eta_1\right) \\ =& \int_0^\infty p\left(g_{11}^2 < \frac{\eta_1\left(1+\alpha_5 g_{15}^2 v + \alpha_6 v x\right)}{\alpha_1 v}\right) f_{g_{16}^2}(x)\, dx \\ =& 1 - \frac{1}{1+\eta_1\left(\frac{\alpha_5 g_{15}^2}{\alpha_1} + \frac{\alpha_6}{\alpha_1}\right)} \exp\left(-\frac{\eta_1}{\alpha_1 u v}\right), \end{aligned} \tag{38}$$

where $u$ is the noise variance, $v = P_u / N_0$ is the SNR.

After getting CDF, we can further get

$$\begin{aligned} p(\theta < \eta) &= \int_0^\eta p\left(\theta_1 < \eta - \left(\theta_2 + x + \theta_4 + \theta_5\right)\right) f_{\theta_3}(x)\, dx \\ &= \int_0^\eta \left(1 - \psi \exp\left(-\frac{\eta - \left(\theta_2 + \theta_3 + \theta_4 + \theta_5\right)}{\alpha_1 u v}\right)\right) f_{\theta_3}\left(\theta_3\right) d\theta_3 \\ &= F_{\theta_3}\left(\theta_3\right)\Big|_0^\eta - \int_0^\eta \psi \exp\left(-\frac{\eta - \left(\theta_2 + \theta_3 + \theta_4 + \theta_5\right)}{\alpha_1 u v}\right) f_{\theta_3}\left(\theta_3\right) d\theta_3, \end{aligned} \tag{39}$$

where

$$\psi = \frac{1}{1 + \eta - \left(\theta_2 + \theta_3 + \theta_4 + \theta_5\right)\left(\frac{\alpha_5 g_{15}^2}{\alpha_1} + \frac{\alpha_6}{\alpha_1}\right)}. \tag{40}$$

We can get

$$p\left(\bar{A}_1\right) = 1 - p(\theta < \eta). \tag{41}$$

## Author contributions

Conceptualization, Shufeng Li; Methodology, Baoxin Su; Supervision, Yao Sun, Sanshan Sun and Libiao Jin; Writing – review & editing, Shufeng Li. All authors have read and agreed to the published version of the manuscript.

## Acknowledgements

This work was supported in part by the National Natural Science Funding of China under Grant 61601414, and in part by the Fundamental Research Funds for the Central Universities.

## Financial disclosure

There are no financial conflicts of interest to disclose. The authors declare no potential conflict of interests.

## References

1. Ding Z, Liu Y, Choi J, et al. Application of Non-Orthogonal Multiple Access in LTE and 5G Networks. *IEEE Communications Magazine* 2017; 55(2): 185-191. doi: 10.1109/MCOM.2017.1500657CM

2. Dai L, Wang B, Yuan Y, Han S, Chih-lin I, Wang Z. Non-orthogonal multiple access for 5G: solutions, challenges, opportunities, and future research trends. *IEEE Communications Magazine* 2015; 53(9): 74-81. doi: 10.1109/MCOM.2015.7263349

3. Cai Y, Qin Z, Cui F, Li GY, McCann JA. Modulation and Multiple Access for 5G Networks. *IEEE Communications Surveys Tutorials* 2018; 20(1): 629-646. doi: 10.1109/COMST.2017.2766698

4. Jacob JL, Abrão T. Nonorthogonal multiple access systems optimization to ensure maximum fairness to users. *Transactions on Emerging Telecommunications Technologies* 2020; 31(4): e3875. doi: https://doi.org/10.1002/ett.3875

5. Basharat M, Ejaz W, Naeem M, Khattak AM, Anpalagan A. A survey and taxonomy on nonorthogonal multiple-access schemes for 5G networks. *Transactions on Emerging Telecommunications Technologies* 2018; 29(1): e3202. e3202 ett.3202doi: https://doi.org/10.1002/ett.3202

6. Zeng M, Yadav A, Dobre OA, Tsiropoulos GI, Poor HV. On the Sum Rate of MIMO-NOMA and MIMO-OMA Systems. *IEEE Wireless Communications Letters* 2017; 6(4): 534-537. doi: 10.1109/LWC.2017.2712149

7. Mahmoud HHH, Amer AA, Ismail T. 6G: A comprehensive survey on technologies, applications, challenges, and research problems. *Transactions on Emerging Telecommunications Technologies* 2021; 32(4): e4233. doi: https://doi.org/10.1002/ett.4233

8. Habibi MA, Nasimi M, Han B, Schotten HD. A Comprehensive Survey of RAN Architectures Toward 5G Mobile Communication System. *IEEE Access* 2019; 7: 70371-70421. doi: 10.1109/ACCESS.2019.2919657

9. Liu X, Ding H, Hu S. Uplink Resource Allocation for NOMA-based Hybrid Spectrum Access in 6G-enabled Cognitive Internet of Things. *IEEE Internet of Things Journal* 2020: 1-1. doi: 10.1109/JIOT.2020.3007017

10. Sun Y, Zhang L, Feng G, Yang B, Cao B, Imran MA. Blockchain-Enabled Wireless Internet of Things: Performance Analysis and Optimal Communication Node Deployment. *IEEE Internet of Things Journal* 2019; 6(3): 5791-5802. doi: 10.1109/JIOT.2019.2905743

11. Chen Y, Bayesteh A, Wu Y, et al. Toward the Standardization of Non-Orthogonal Multiple Access for Next Generation Wireless Networks. *IEEE Communications Magazine* 2018; 56(3): 19-27. doi: 10.1109/MCOM.2018.1700845

12. Tang W, Kang S, Ren B. Performance Analysis of Cooperative Pattern Division Multiple Access (Co-PDMA) in Uplink Network. *IEEE Access* 2017; 5: 3860-3868. doi: 10.1109/ACCESS.2017.2683531

13. Xu J, Han X, Ding H, Li Z, Yu Z, Dai X. Optimisation of convergence-aware coded PDMA for 5G wireless systems. *IET Communications* 2019; 13(2): 243-250. doi: https://doi.org/10.1049/iet-com.2018.5429

14. Ren B, Wang Y, Kang S, et al. Link Performance Estimation Technique for PDMA Uplink System. *IEEE Access* 2017; 5: 15571-15581. doi: 10.1109/ACCESS.2017.2728685

15. Ren B, Wang Y, Dai X, Niu K, Tang W. Pattern matrix design of PDMA for 5G UL applications. *China Communications* 2016; 13(Supplement2): 159-173. doi: 10.1109/CC.2016.7833470

16. Sun J, Wang C, Zeng J, Su X, Lv T. Design of PDMA Pattern Matrix in 5G Scenarios. *2020 IEEE 91st Vehicular Technology Conference (VTC2020-Spring)* ; 2020: 1-6 doi: 10.1109/VTC2020-Spring48590.2020.9129446

17. Doğan S, Tusha A, Arslan H. NOMA With Index Modulation for Uplink URLLC Through Grant-Free Access. *IEEE Journal of Selected Topics in Signal Processing* 2019; 13(6): 1249-1257. doi: 10.1109/JSTSP.2019.2913981

18. Hasan SM, Mahata K, Hyder MM. Uplink Grant-Free NOMA With Sinusoidal Spreading Sequences. *IEEE Transactions on Communications* 2021; 69(6): 3757-3770. doi: 10.1109/TCOMM.2021.3062389

19. Shahab MB, Abbas R, Shirvanimoghaddam M, Johnson SJ. Grant-Free Non-Orthogonal Multiple Access for IoT: A Survey. *IEEE Communications Surveys Tutorials* 2020; 22(3): 1805-1838. doi: 10.1109/COMST.2020.2996032

20. Abbas R, Shirvanimoghaddam M, Li Y, Vucetic B. A Novel Analytical Framework for Massive Grant-Free NOMA. *IEEE Transactions on Communications* 2019; 67(3): 2436-2449. doi: 10.1109/TCOMM.2018.2881120

21. Lai K, Lei J, Deng Y, Wen L, Chen G, Liu W. Analyzing Uplink Grant-free Sparse Code Multiple Access System in Massive IoT Networks. *IEEE Internet of Things Journal* 2021: 1-1. doi: 10.1109/JIOT.2021.3109912

22. Turyn R. Ambiguity functions of complementary sequences (Corresp.). *IEEE Transactions on Information Theory* 1963; 9(1): 46-47. doi: 10.1109/TIT.1963.1057807

23. Liu T, Xu C, Li Y. Multiple Complementary Sequence Sets With Low Inter-Set Cross-Correlation Property. *IEEE Signal Processing Letters* 2019; 26(6): 913-917. doi: 10.1109/LSP.2019.2902752

24. Lu L, Dubey VK. Performance of a Complete Complementary Code-Based Spread-Time CDMA System in a Fading Channel. *IEEE Transactions on Vehicular Technology* 2008; 57(1): 250-259. doi: 10.1109/TVT.2007.905331

25. Qi L, Yao Y, Wu G. Radar and communication integration based on complete complementary codes. *The Journal of Engineering* 2019; 2019(21): 7730-7733. doi: https://doi.org/10.1049/joe.2019.0754

26. Khirallah C, Stankovic V, Stankovic L, Yang Y, Xiong Z. Bandwidth efficient multi-station wireless streaming based on complete complementary sequences. *IEEE Transactions on Wireless Communications* 2009; 8(2): 552-556. doi: 10.1109/TWC.2009.070958

27. Mounir M, El Mashade MB, Mohamed Aboshosha A. On The Selection of Power Allocation Strategy in Power Domain Non-Orthogonal Multiple Access (PD-NOMA) for 6G and Beyond. *Transactions on Emerging Telecommunications Technologies*; n/a(n/a): e4289. doi: https://doi.org/10.1002/ett.4289

28. Farhadi Zavleh A, Bakhshi H. Resource allocation in sparse code multiple access-based systems for cloud-radio access network in 5G networks. *Transactions on Emerging Telecommunications Technologies*; 32(1): e4153. doi: https://doi.org/10.1002/ett.4153

29. Qureshi S, Hassan SA, Jayakody DNK. Divide-and-allocate: An uplink successive bandwidth division NOMA system. *Transactions on Emerging Telecommunications Technologies* 2018; 29(1): e3216. e3216 ett.3216doi: https://doi.org/10.1002/ett.3216

30. Baidas MW, Bahbahani Z, El-Sharkawi N, Shehada H, Alsusa E. Joint relay selection and max-min energy-efficient power allocation in downlink multicell NOMA networks: A matching-theoretic approach. *Transactions on Emerging Telecommunications Technologies* 2019; 30(5): e3564. e3564 ett.3564doi: https://doi.org/10.1002/ett.3564

31. Zeng J, Fan X, Zhong Y, Peng M, Lv T, Jiang T. Downlink Power Allocation Optimization in Pattern Division Multiple Access. *IEEE Access* 2021; 9: 14649-14659. doi: 10.1109/ACCESS.2021.3049493

32. Ren B. Research on Key Technologies of pattern division non orthogonal multiple access (PDMA) for 5g. PhD thesis. *Beijing University of Posts and Telecommunications* 2017; doi: CNKI:CDMD:1.1017.289460

33. Yang Z, Xu P, Ahmed Hussein J, Wu Y, Ding Z, Fan P. Adaptive Power Allocation for Uplink Non-Orthogonal Multiple Access With Semi-Grant-Free Transmission. *IEEE Wireless Communications Letters* 2020; 9(10): 1725-1729. doi: 10.1109/LWC.2020.3002800

34. Sun Y, Qin S, Feng G, Zhang L, Imran MA. Service Provisioning Framework for RAN Slicing: User Admissibility, Slice Association and Bandwidth Allocation. *IEEE Transactions on Mobile Computing* 2021; 20(12): 3409-3422. doi: 10.1109/TMC.2020.3000657

35. Das S, Budišin S, Majhi S, Liu Z, Guan YL. A Multiplier-Free Generator for Polyphase Complete Complementary Codes. *IEEE Transactions on Signal Processing* 2018; 66(5): 1184-1196. doi: 10.1109/TSP.2017.2780050

36. Jun S, Kang Y, Kim J, Kim C. Ultra-low-latency services in 5G systems: A perspective from 3GPP standards. *ETRI Journal* 2020; 42(5): 721-733. doi: https://doi.org/10.4218/etrij.2020-0200

37. Li Ping , Lihai Liu , Keying Wu , Leung WK. Interleave division multiple-access. *IEEE Transactions on Wireless Communications* 2006; 5(4): 938-947. doi: 10.1109/TWC.2006.1618943

38. Sun Y, Jiang W, Feng G, et al. Efficient Handover Mechanism for Radio Access Network Slicing by Exploiting Distributed Learning. *IEEE Transactions on Network and Service Management* 2020; 17(4): 2620-2633. doi: 10.1109/TNSM.2020.3031079

**How to cite this article:** Shufeng Li., Baoxin Su, Yao Sun, Sanshan Sun, and Libiao Jin (2021), Uplink Grant-free PDMA Transmission Scheme by Exploiting Poly Complementary Sequence, *Q.J.R. Meteorol. Soc.*, *2021;XX:X–X.*